Divertor IR thermography on Alcator C-Mod[a)]

J. L. Terry,[1,b)] B. LaBombard,[1] D. Brunner,[1] J. Payne,[1] and G. A. Wurden[2]
[1]*Plasma Science and Fusion Center, MIT, Cambridge, Massachusetts 02139, USA*
[2]*Los Alamos National Laboratory, Los Alamos, New Mexico 87545, USA*

(Presented 20 May 2010; received 17 May 2010; accepted 21 June 2010; published online 6 October 2010)

Alcator C-Mod is a particularly challenging environment for thermography. It presents issues that will similarly face ITER, including low-emissivity metal targets, low-Z surface films, and closed divertor geometry. In order to make measurements of the incident divertor heat flux using IR thermography, the C-Mod divertor has been modified and instrumented. A 6° toroidal sector has been given a 2° toroidal ramp in order to eliminate magnetic field-line shadowing by imperfectly aligned divertor tiles. This sector is viewed from above by a toroidally displaced IR camera and is instrumented with thermocouples and calorimeters. The camera provides time histories of surface temperatures that are used to compute incident heat-flux profiles. The camera sensitivity is calibrated *in situ* using the embedded thermocouples, thus correcting for changes and nonuniformities in surface emissivity due to surface coatings. © *2010 American Institute of Physics.* [doi:10.1063/1.3478669]

I. INTRODUCTION

Power handling is one of the primary functions—and most challenging problems—for a tokamak divertor. IR thermography is an important tool that can quantify heat-flux "footprints" at divertor targets.[1–5] On ITER, IR thermography is to be used as the primary diagnostic for a number of important measurements, including

- heat-load profiles on the divertor target plates,
- maximum divertor surface temperature, and
- first-wall surface temperatures.

To make the divertor measurements, IR diagnostics within a divertor cassette,[6] as well as divertor imaging by IR and visible systems from the upper vacuum chamber ports are planned. Six of the upper ports are to hold periscope modules that view target sections that are displaced toroidally from the periscopes. An initial design[7] for this "top-viewing" system has been performed. C-Mod has recently upgraded its divertor IR thermography and its capabilities for measuring the divertor heat loads and heat-flux profiles on the targets. In the process, we found a number of challenging issues that will also be faced when making similar measurements on ITER. These issues and our experience in addressing them are the primary subject of this report. The shared issues include the following:

- grazing angles of incidence for magnetic field lines intersecting the targets,
- closed divertor geometry with near vertical targets,
- oblique observation angles when viewing from above,
- shiny, low emissivity refractory targets (W for ITER, Mo and W for C-Mod),
- possible movement or shaking of the image during operation,
- low-Z surface films, changing with time, and
- extremely high peak heat fluxes.

II. IR CAMERA AND PERISCOPE

The IR camera used for the divertor thermography on C-Mod [FLIR Titanium SC7000 (Ref. 8)] detects emission in the 3–5 μm bandpass with 320×256 pixel resolution. The InSb-based detector is cooled to 73 K, and full-frames can be read out at a rate of up to 383 frames/s, with integration times, τ_{int}, which are set independently of the frame rate. The camera is housed in soft-iron magnetic shield box mounted on the top of a concrete "igloo" that surrounds C-Mod. The box is water-cooled to a temperature of 12–15 °C. The camera-body is thermally connected to the box using thermal gel packs, and thus it and its input lens are provided with a stable cool environment. The camera-body temperature is monitored and reported with each data acquisition cycle. This is important because a small but non-negligible amount of detected emission comes from the body and input optics.

Laboratory "bench" calibrations with the camera show that clean heated Mo target tiles emit as graybodies. We assume that the tiles of both the viewed first-wall and divertor surfaces remain graybodies. We also assume that the camera-body/lens/periscope system emits as a graybody. Thus the detected signal, S, is parametrized as

$$S(T_{surf}T_{body},\tau_{int}) = \text{offset}(\tau_{int}) + \alpha(\tau_{int})B(T_{body}) + \beta(\tau_{int})B(T_{surf}), \quad (1)$$

where B(T) is the blackbody emission[9] within the spectral bandpass of the camera for a temperature T, α is a constant

[a)]Contributed paper, published as part of the Proceedings of the 18th Topical Conference on High-Temperature Plasma Diagnostics, Wildwood, New Jersey, May 2010.
[b)]Author to whom correspondence should be addressed. Electronic mail: terry@psfc.mit.edu.

times τ_{int} (determined by varying T_{body} while viewing a cold plate), and β is a calibration parameter (also linear in τ_{int}) that depends on the viewed surface emissivity, the periscope transmission, the detector sensitivity, and the angle with which the surface is viewed. It can be different for each pixel and is determined as described in Sec. III. Offset(τ_{int}) is an experimentally determined parameter dependent only upon τ_{int}. Since the temperature of the viewed surface, T_{surf}, is the desired quantity, Eq. (1) is recast as

$$T_{surf} = B^{-1}\{[S(T_{surf}T_{body}, \tau_{int}) - \text{Offset}(\tau_{int}) - \alpha(\tau_{int})B(T_{body})]/\beta(\tau_{int})\}, \quad (2)$$

where B^{-1} is the inverse of the blackbody function and all quantities on the right-hand-side are known.

An approximately 36° toroidal section of the outer divertor structure is viewed through an ~5 m long periscope.[10] One length of periscope optics is inserted into an ~2 m long reentrant tube secured to the tokamak structure. Other sections of the periscope and the camera are securely mounted on the C-Mod igloo. The periscope presents an image to the IR camera. Because of small relative motions between the tokamak and camera during the time the magnetic field coils are energized (and especially during plasma disruptions), the image measured by the camera shakes frame-to-frame. (τ_{int} is typically 150 μs and there is no frame-smearing. Typical frame-to-frame times are 10 ms.) The camera image shakes by tens of pixels during this time. Since stabilization and registration of the image at the single pixel level are crucial for quantitative thermography, image-stabilization algorithms have been developed and are run between shots. These algorithms depend on maximizing the cross-correlation between edge-detecting[11] filtered images and a reference image that has also been filtered with the edge-detecting operator. Most of the edges in the C-Mod images are provided by the target tiles themselves. However, for future campaigns, we are modifying a few of the viewed tiles by cutting a simple pattern on them, thus providing a unique pattern of edges in the images to "lock" onto. Registration of view is accomplished by constructing a wire-mesh computer representation of the objects that are visible in the field-of-view (e.g., the target tiles) and by projecting it onto the camera's image plane. Typical spatial resolution at the divertor target ranges from 1 to 3 mm/pixel, and features (e.g., tile gaps) of ~2 mm size are evident in the images.

III. THERMOGRAPHY ISSUES

A. Grazing field line angles

The field lines striking perfectly aligned outer divertor targets in C-Mod would do so at angles between 0.5° and 1.5°. However, the outer divertor sections are not perfectly aligned, and the combination of grazing field line angles and imperfectly aligned targets results in strong heating of leading edges, asymmetric heat loads, and shadowing of some target surfaces. In order to make valid measurements of the parallel heat flux onto the targets, we have installed within the field-of-view of the IR periscope, a 6° toroidal section of the outer divertor that has a 2° toroidal ramp. Thus by construction, this ramped section is not shadowed. The ramped section has been instrumented with calorimeters, surface thermocouples, and thermocouples embedded within the target tiles.

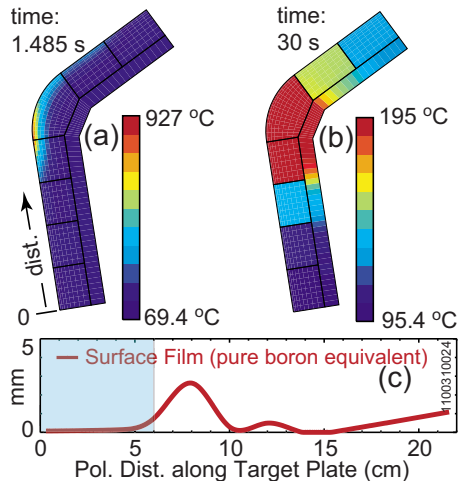

FIG. 1. (Color online) (a) Cross-section of the outer target with temperatures, as modeled by a 2D heat-transport code using IR thermography inputs, 1.485 s into the discharge. (b) Same as (a) but ~28 s after discharge termination. (c) Effective surface coating thickness of B needed to eliminate negative heat fluxes. (In the shaded region, the heat fluxes are too small to derive an effective thickness.)

B. Viewing issues

A cross-section of C-Mod's outer divertor target is shown in Fig. 1. When the targets are viewed from above, the closed divertor geometry and near-vertical plate necessitate that the view from above be displaced toroidally. In C-Mod, the viewing angles of the target are large, ranging from 35° to 80° away from normal to the target surfaces. Our bench calibrations show that the emissivity from a clean Mo divertor tile increases sharply as the view angle increases beyond about 55°. While this effect is present in the measurements on the tokamak, another source for significant variation in surface emissivity is also present, i.e., changing low-Z surface coatings (e.g., boron). A clean Mo target surface has a low emissivity (~0.2), and the coatings increase the emissivity significantly, making *in situ* calibrations necessary. Additionally, we observe nonthermal emissions (both from the plasma and as a result of reflections from the relatively shiny Mo surfaces) that sometimes contaminate the measurement of surface emission. To correct for these effects, we subtract the nonthermal emission by measuring emission from target regions that are shadowed (by the toroidally ramped section) from the plasma heat flux.

C. Calibration and surface coatings

As noted above, the divertor target surfaces do not remain clean Mo in the tokamak environment. Different surface coatings are produced by periodic boronizations and by plasma surface interactions with both tokamak plasmas and daily preoperation "discharge cleaning" plasmas. As a result, the bench calibrations using clean, heated Mo tiles that relate detected IR intensity to Mo tile surface temperature and viewing angle [i.e., that determine the β's of Eq. (1)] did *not* produce accurate target temperatures. Thus the needed sensi-

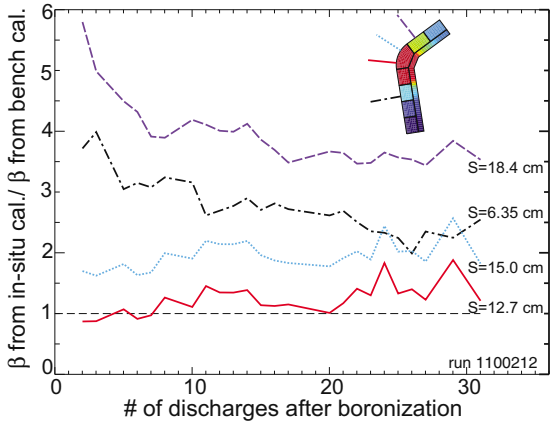

FIG. 2. (Color online) Changes in the β calibration factors [Eq. (1)] for different points up the divertor target as a function of the number of tokamak discharges after a boronization. The *in situ* β's are compared to the clean-Mo bench calibrations. S is the poloidal distance up along the surface, locations noted on inset.

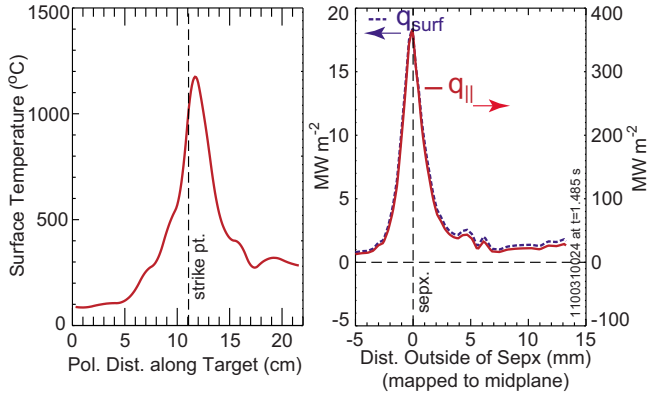

FIG. 3. (Color online) (Left) Profiles of surface temperature profiles and (right) derived parallel heat flux and surface-normal heat flux (mapped to the midplane) during a period of H-mode confinement.

tivity calibrations are produced after each tokamak pulse by taking IR camera data and tile thermocouple data for at least 25 s after the discharge termination, at which time the individual tiles have thermally equilibrated, as shown in Fig. 1(b). 25–30 s after the discharge the tiles are still hot and values for β [Eq. (1)] are chosen such that the intensity-derived temperatures are those measured by the thermocouples.[12] Thus, although the spatial density and time resolution of the thermocouples is not large enough to provide detailed heat-flux footprints and time histories, they are *crucial* for the thermography since they provide *in situ* intensity-sensitivity calibrations for the IR system, which does have the spatial and temporal resolution needed for the surface-temperature and heat-flux profile measurements. To illustrate the importance of the *in situ* calibration and the effects of changing surface coatings, we plot (Fig. 2) the ratio of the *in situ* β calibration factors to the clean-Mo bench-calibration factors at four points on the ramped target tiles as a function of the number of tokamak discharges after a typical overnight boronization. (Boronization[13] applies surface coatings of boron to the vacuum surfaces.) Three important effects are evident: (1) The clean-Mo calibration cannot be relied upon to yield accurate surface temperatures after boronization and exposures to tokamak plasmas. (2) The boronization coatings on the targets increase the emissivity of the surfaces and the coatings are changed by exposure to tokamak plasmas. (3) In the high heat-flux/strike point regions, the coating appears to be removed rapidly, whereas in regions of lower heat flux the coating removal never appears to be complete, but yields a steady-state emissivity of 5–10 discharges after boronization. Note that the *in situ* calibration also compensates for any changes in vacuum-window transmission or first-mirror reflectivity.

The surface emission is not the only thing complicated by changing surface coatings. The thermal conductivity of the coating is important for modeling the thermal transport and producing heat-flux footprints. Following Refs. 14 and 3, this effect is included in the two-dimensional (2D) heat-transport model by adjusting the thickness of an assumed "boron" coating until physically unrealistic negative heat fluxes in response to changing measured surface temperatures are eliminated. The assumption that the coating is boron is irrelevant for the resulting heat fluxes. A typical result for the coating "thickness" needed in the model is shown in Fig. 1(c). For this and most other plasmas during the run campaign of this investigation, the strike point was maintained (during the high-power heating times) between 10 and 15 cm up the plate, where the implied coating thickness is small. Qualitatively, the results for the increases in the *in situ* β calibration factors above the clean-Mo calibrations (Fig. 2) trend with the coating thicknesses needed to eliminate the negative heat fluxes.

IV. HEAT-FLUX PROFILES

The goal of C-Mod's IR thermography is to measure surface temperature profiles, and from those derive heat-flux profiles. After addressing the issues discussed above, this is now being done routinely on C-Mod. Examples of these profiles are shown in Fig. 3. Peak surface-normal heat fluxes greater than 15 MW/m^2, corresponding to parallel heat fluxes >300 MW/m^2, are typical in both high confinement H-modes and rf-heated, low-confinement L-modes. Surface temperatures in excess of 1000 °C are often measured on the ramped tiles. The heating of the targets at the same time of the profiles of Fig. 3 as modeled by the heat-transport code is shown in Fig. 1(a). These profiles illustrate the last of the issues listed in Sec. I, i.e., the high parallel (to the magnetic field) heat fluxes on C-Mod. Other important physical quantities are evident in the profiles. For example, the measured widths of the main peak of the heat-flux profiles (full-width-half-maximum=2.0 mm in the Fig. 3 profile) constrain the major radius and magnetic field dependencies of multimachine empirical scaling relations for the scrape-off layer (SOL) heat-flux widths.[15,16] Also evident in the heat-flux profiles is a far-SOL "tail" with constant or slowly decreasing heat flux. The existence of this tail has been confirmed Langmuir probes mounted in other divertor tiles.

The calorimeters and thermocouples embedded in the viewed ramped tiles also provide important checks on the surface-temperature time-history inputs to the heat-transport analysis of the target (including the assumption that the target surfaces are graybodies), as well as checks on the analy-

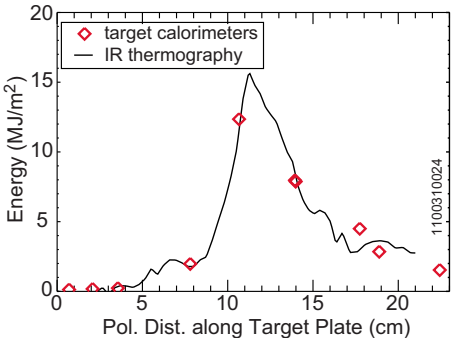

FIG. 4. (Color online) Comparison of the energy deposited on the target as measured using thermography and as measured by the calorimeters mounted in the target tiles.

sis itself. The incident energies associated with the IR temperature time histories are compared to those measured by the calorimeters. Typically agreement between the two measurements is good, as is shown in Fig. 4. Another check is provided when the measured IR surface-temperatures are imposed in the 2D heat-transport model *only for the plasma pulse duration*. Then, after continuing the model calculation past the time needed for the individual tiles to equilibrate, the computed tile temperature rise is compared to (and should equal) the rise measured by the embedded thermocouples. We find in performing this check that the target heat-transport model typically underestimates the temperature rise (~30 s after the discharge) for the tile(s) that received the peak heat flux by 10%–20%. For the other target tiles the agreement is good. The reason for the disagreement on the peak-heat-flux tiles is still under investigation.

ACKNOWLEDGMENTS

The authors thank Istvan Cziegler for his numerical fit of the inverse blackbody function. This work is supported by DoE Award Nos. DE-FC02-99ER54512 and DE-AC52-06NA25396.

[1] A. Herrmann, W. Junker, K. Gunther, S. Bosch, M. Kaufmann, J. Neuhauser, G. Pautasso, Th. Richter, and R. Schneider, Plasma Phys. Controlled Fusion **37**, 17 (1995).
[2] C. J. Lasnier, D. N. Hill, T. W. Petrie, A. W. Leonard, T. E. Evans, and R. Maingi, Nucl. Fusion **38**, 1225 (1998).
[3] P. Andrew, J. P. Coad, T. Eich, E. Gauthier, A. Herrmann, G. F. Matthews, V. Riccardo, M. Stamp, and Contributors to EFDA-JET Work Programme, J. Nucl. Mater. **313–316**, 135 (2003).
[4] T. Eich, A. Herrmann, P. Andrew, A. Loarte, and Contributors to EFDA-JET Program, J. Nucl. Mater. **313–316**, 919 (2003).
[5] R. Reichle, D. Guilhem, R. Mitteau, J. C. Vallet, C. Balorin, P. Bibet, M. Chantant, E. Delchambre, C. Desgrange, L. Ducobu, A. Ekedahl, F. Escourbiac, F. Faisse, A. Geraud, M. Goniche, M. Jouve, M. Lipa, G. Martin, P. Messina, D. Moulin, C. Pocheau, H. Roche, A. Saille, F. Saint-Laurent, J. Schlosser, E. Thomas, and E. Tsitrone, Nucl. Fusion **43**, 797 (2003).
[6] R. Reichle, Ph Andrew, C. Balorin, B. Brichard, S. Carpentier, Y. Corre, M. Davi, R. Daviot, C. Desgranges, J. L. Gardarein, E. Gauthier, D. Guilhem, S. Gicquel, A. Herrmann, D. Hernandez, M. Jouve, Ch. Le Niliot, Th. Loarer, A. Martin, J. P. Martins, J.-B. Migozzi, J. P. Patterlini, C. Pocheau, F. Rigollet, H. Roche, and J. M. Travere, J. Nucl. Mater. **390–391**, 1081 (2009).
[7] C. J. Lasnier, L. G. Seppala, K. Morris, M. Groth, M. E. Fenstermacher, S. L. Allen, E. Synakowski, and J. Ortiz, "Visible and infrared optical design for the ITER upper ports" in http://www.pppl.gov/usiter-diagnostics/Instrumentation-Packages/Upper-IR-Visible-Cameras/ICP006779-A ITER Camera Report (LLNL).pdf (2007).
[8] Previously sold by CEDIP Infrared Systems as the Titanium 550M camera.
[9] W. K. Widger, Jr. and M. P. Woodall, Bull. Am. Meteorol. Soc. **57**, 1217 (1976).
[10] R. J. Maqueda, G. A. Wurden, J. L. Terry, and J. A. Stillerman, Rev. Sci. Instrum. **70**, 734 (1999).
[11] The Sobel operator is used for the edge detection.
[12] In fact, a heat-transport model of the thermocouple response shows that the thermocouples have not yet equilibrated with bulk tiles surrounding them. The temperatures used to calibrate the IR thermography are corrected for this effect and thus are not exactly the measured thermocouple temperatures. The time response of the thermocouples will be improved for the next set of experiments.
[13] B. Lipschultz, D. A. Pappas, B. Labombard, J. E. Rice, D. Smith, and S. J. Wukitch, Nucl. Fusion **41**, 585 (2001).
[14] A. Herrmann, Proceedings of the 28th EPS Conference on Controlled Fusion and Plasma Physics, Madeira, 2001.
[15] G. Kirnev, W. Fundamenski, and G. Corrigan, Plasma Phys. Controlled Fusion **49**, 689 (2007).
[16] A. Loarte, S. Bosch, A. Chankin, S. Clement, A. Herrmann, D. Hill, K. Itami, J. Lingertat, B. Lipschultz, K. McCormick, R. Monk, G. D. Porter, M. Shimada, M. J. Sugihara, J. Nucl. Mater. **266-269**, 587 (1999).